



Cite this: *Chem. Soc. Rev.*, 2026, 55, 1915

## Cyclopropane-to-organoboron conversion via C–H and C–C bond activation

Shuyu Kang,<sup>†</sup> Xueli Lv<sup>†</sup> and Zhuangzhi Shi \*

Organoborons have emerged as a class of privileged building blocks in modern organic synthesis, enabling unparalleled molecular diversity and serving as versatile carboxylic acid bioisosteres with profound implications in drug discovery. Concurrently, cyclopropanes have garnered sustained attention as unique synthetic platforms, with their rigid and highly strained three-membered ring structures conferring distinctive steric and electronic properties that facilitate selective C–H and C–C activation processes. The strategic transformation of cyclopropanes into organoborons represents a particularly appealing synthetic approach, offering access to valuable molecular architectures. This review systematically examines the seminal advancements of cyclopropane-to-organoboron conversion over recent years, employing a structured classification based on two fundamental activation modes: C–H borylation and C–C borylation. The review provides in-depth mechanistic elucidation, with particular emphasis on catalytic cycles, key reactive intermediates, and stereodiscrimination processes, thereby offering fundamental insights into the governing principles of these transformations. Looking forward, continued innovation in catalyst design and the exploration of novel reaction pathways are anticipated to significantly expand the synthetic utility and scope of conversions, potentially opening new frontiers in organic synthesis and medicinal chemistry.

Received 2nd July 2025

DOI: 10.1039/d5cs00759c

[rsc.li/chem-soc-rev](https://rsc.li/chem-soc-rev)

### Key learning points

- (1) Highlight the strategic significance of cyclopropane-to-organoboron conversion in advancing organic synthesis and drug discovery frontiers.
- (2) Discern the applicable cyclopropane types for organoboron preparation and grasp their inherent characteristics and reactivities.
- (3) Reveal the intricate mechanisms, influencing elements, and practical applications of cyclopropane C–H activation in organoboron synthesis.
- (4) Probe into the specific procedures, reaction intermediates, and product selectivities during cyclopropane C–C activation for organoboron generation.
- (5) Evaluate the current limitations and challenges of cyclopropane-to-organoboron conversion and project its future developmental trajectories.

## 1. Introduction

Cyclopropane, a deceptively simple molecule, holds significant importance in organic chemistry due to its highly strained three-membered ring structure.<sup>1–4</sup> This unique architecture, akin to a tightly coiled spring, is the foundation of its exceptional chemical reactivity.<sup>5,6</sup> Cyclopropane units frequently serve as key structural motifs in natural products and pharmaceuticals (for selected examples, see Fig. 1).<sup>7</sup> For example, they can enhance antibiotic activity by improving target binding or modulate biological activity in drug molecules by influencing conformation and receptor interactions. Their controlled

flexibility also allows for better fit within protein active sites. Such properties of cyclopropane, from its strained ring structure to its versatile role in modulating biological activity, make it an indispensable component in the realm of organic chemistry.

Well-established methods exist for their preparation, often under mild conditions with good functional group tolerance (Fig. 2). Synthetic strategies for cyclopropane derivatives can generally be classified into three main categories: [2+1] cycloaddition of carbenes with alkenes, such as Simmons–Smith reaction,<sup>8</sup> ring-contraction reactions,<sup>9</sup> and ring-closing cyclopropanation of acyclic precursors, such as the Corey–Chaykovsky reaction.<sup>10</sup> In addition to these principal approaches, other useful routes include functionalization of cyclopropenes,<sup>11</sup> contraction of cyclobutenes,<sup>12</sup> the use of cyclopropyl Grignard reagents or cyclopropyl halides,<sup>13,14</sup> and the Kulinkovich reaction employing esters or amides with Grignard reagents.<sup>15</sup> Given their diverse

State Key Laboratory of Coordination Chemistry, Chemistry and Biomedicine Innovation Center (ChemBIC), School of Chemistry and Chemical Engineering, Nanjing University, Nanjing 210093, China. E-mail: shiz@nju.edu.cn

<sup>†</sup> These authors contributed equally to this work.



synthetic accessibility, ease of derivatization, and unique strain-driven reactivity, cyclopropanes are ideal substrates for further functionalization.

Organoborons hold a position of paramount importance across numerous domains of chemical science.<sup>16</sup> In the pharmaceutical industry, the integration of boron groups has spurred the advancement of a multitude of contemporary drugs (Fig. 3).<sup>17</sup> Specifically, in the realm of anticancer agents, the boron group can be meticulously designed to engage with specific cancer-related proteins. This interaction disrupts the normal function of these proteins, thereby effectively inhibiting tumor growth. In the case of antibacterial drugs, boron-containing compounds can target unique bacterial enzymes. This provides novel strategies for combating drug-resistant bacteria. In synthetic chemistry, which serves as the cornerstone for constructing complex organic molecules, organoboronates assume a central role. They are capable of forming C–C and C–heteroatom bonds with high precision, making them

reliable building blocks in the synthesis of a wide variety of organic compounds.

The synthesis of organoboron compounds continues to be a pivotal area in organic chemistry, driven by their extensive applications.<sup>18,19</sup> Among the established methodologies, the Brown hydroboration of olefins is particularly notable for its classic *anti*-Markovnikov transformation (Fig. 4A).<sup>20</sup> This reaction features the simultaneous addition of hydrogen and boron atoms to the same face of the double bond *via* a four-membered concerted transition state. In contrast, the conversion of cyclopropanes to organoboron compounds introduces greater complexity and diversity, presenting both challenges and opportunities. Historically, cyclopropane borylation relied on pre-functionalized substrates like cyclopropyl halides or Grignard reagents.<sup>21,22</sup> They were often limited by a narrow substrate scope, restricting the variety of cyclopropane derivatives that could be effectively utilized. Recent advancements have significantly expanded the synthesis of organoboron compounds from cyclopropanes through the activation of C–H and C–C bonds (Fig. 4B). However, achieving precise selectivity in these transformations remains a critical challenge. This includes differentiating between C–H and C–C activation and controlling the selectivity of distal and proximal  $\sigma$ -bonds within the cyclopropane ring. Through innovative strategies such as catalyst design, the use of directing groups, and the development of novel reaction systems, it is now possible to selectively synthesize a diverse range of organoboron compounds from cyclopropanes.

This review aims to comprehensively cover the two main strategies for the cyclopropane-to-organoboron conversion: C–H borylation and C–C borylation. Given the vast number of C–C activation cases, we have further subclassified these reactions based on the types of cyclopropanes involved: (1) alk(en/yn)lycyclopropanes; (2) *gem*-difluorocyclopropanes;



Shuyu Kang

*Shuyu Kang was born in Henan Province, People's Republic of China, in 1997. He received his BS degree from Zhengzhou University in 2020. He then moved to Nanjing University, where he is currently pursuing his PhD under the supervision of Prof. Zhuangzhi Shi. His current research focuses on boron chemistry.*



Xueli Lv

*Xueli Lv was born in Shandong province, People's Republic of China, in 1995. She received her BS and MS degrees in chemistry and organic chemistry from Qingdao University of Science & Technology and Nankai University in 2017 and 2020. Then, she moved to Nanjing University and completed her PhD in organic chemistry with Prof. Zhuangzhi Shi. Her current research efforts are focused on asymmetric C–H activation.*



Zhuangzhi Shi

*Zhuangzhi Shi was born in Jiangsu province, People's Republic of China, in 1983. He received his BS and MS degrees in chemistry and organic chemistry from Yangzhou University in 2005 and 2008. Then, he moved to Peking University and completed his PhD in medicinal chemistry with Prof. Ning Jiao. In 2011, he joined the group of Prof. Frank Glorius at Munster University (Germany), as an Alexander von Humboldt*

*Research Fellow. In 2014, he joined the Department of Chemistry at Nanjing University as a full professor. His current research efforts are focused on synthetic methodology, including the activation of inert chemical bonds, main group chemistry and asymmetric catalysis.*





Fig. 1 Selective examples of cyclopropane-based drugs and natural products.



Fig. 2 Methods for the synthesis of cyclopropanes.

(3) aminocyclopropanes; (4) iminocyclopropanes; (5) simple cyclopropanes. For each category, we will not only examine the reaction inception and evolution but also delve into the scope and limitations. We will support our analysis with representative reaction pathways derived from experimental data and density functional theory (DFT) calculations. In the concluding section, we will highlight the remaining challenges and opportunities in this field. By identifying the areas that require further breakthroughs, we hope to provide a clear roadmap for future research endeavors, inspiring scientists to continue exploring the fascinating intersection of cyclopropane and boron chemistry.

## 2. C–H borylation of cyclopropanes

Compared with traditional C–H borylation substrates such as arenes, alkenes, and linear alkanes, cyclopropanes represent a particularly intriguing class of aliphatic substrates owing to their distinctive bonding framework and pronounced ring

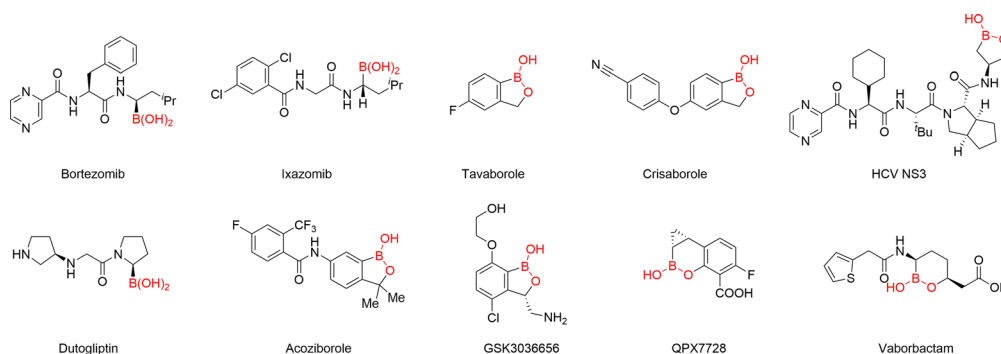


Fig. 3 Selective examples of organoboron-based biologically and pharmacologically active molecules.





Fig. 4 (A) Classical hydroboration of alkenes with borane reagents. (B) Modern strategies for synthesis of organoboron compounds from cyclopropanes by C–H and C–C activation.

strain.<sup>23</sup> The planar arrangement of the three carbon atoms imposes severe angular strain ( $60^\circ$  bond angles), coupled with torsional strain from the eclipsed C–H bonds. As a result, the C–C bonds exhibit substantial  $\pi$ -character and behave more like C=C bonds, whereas the C–H bonds display greater  $\sigma$ -character, shorter bond lengths, and higher bond dissociation energies ( $106 \text{ kcal mol}^{-1}$ ) compared with typical alkanes ( $101 \text{ kcal mol}^{-1}$  for the C–H bond in ethane).<sup>24</sup> These structural and electronic features render C–H borylation of cyclopropanes especially challenging, yet the resulting borylated cyclopropanes can participate in diverse, high-value transformations, offering significant opportunities for molecular diversification and synthetic innovation.

Early borylation strategies relied on pre-functionalized cyclopropanes, such as halides or organometallics, often requiring stoichiometric metal reagents.<sup>25</sup> While effective, these approaches offer limited substrate scope and raise sustainability concerns. In contrast, transition metal-catalyzed C–H borylation of cyclopropanes has emerged as a more direct and versatile alternative. Leveraging the ring strain and rigidity of the three-membered scaffold, these reactions enable site-selective functionalization without prior activation, providing efficient access to structurally defined organoboron compounds.

Among the various transition metal systems explored for C–H borylation, iridium catalysis has proven particularly effective.<sup>26</sup> In 2013, Hartwig and colleagues reported an Ir-catalyzed borylation of C–H bonds in cyclopropanes using  $\text{B}_2\text{pin}_2$  (Scheme 1).<sup>27</sup> Considering the broad utility of the 4,4'-dtbpy/Ir catalyst combination in aromatic C–H activation, the authors conducted a bidentate nitrogen ligand screen that identified **L1** as the optimal ligand for this system and subsequently refined the reaction conditions through solvent evaluation. The reaction was also shown to be compatible with a more accessible catalyst,  $[\text{Ir}(\text{cod})(\text{OMe})_2]$ , albeit at the cost of slightly reduced yields. Notably, substrates having bulkier groups such as bromo or carbonyl groups exhibited higher diastereoselectivity compared to those containing less hindered groups like nitrile. The resulting boryl cyclopropanes act as versatile synthetic intermediates, as they can be readily converted into a range of derivatives, including trifluoroborate salts, boronic acids, and hydroxylated products. Furthermore, the cyclopropylboronate ester bearing a carbonyl



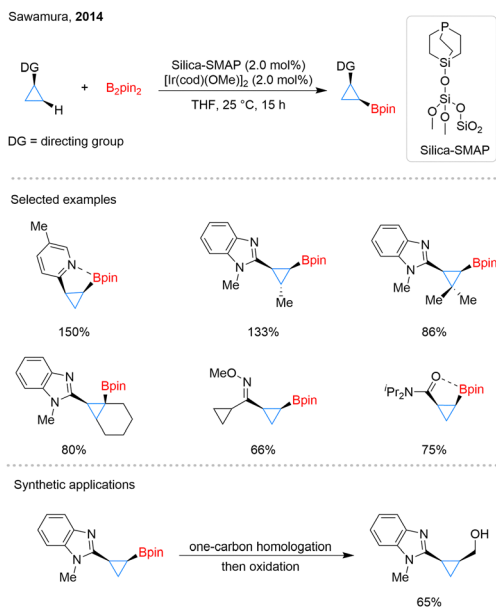
Scheme 1 Iridium-catalyzed C–H borylation of cyclopropanes.

substituent was found to undergo Suzuki–Miyaura cross-coupling in a moderate yield.

One year later, Sawamura and his team developed silica-supported monophosphane–Ir catalyst systems (Scheme 2).<sup>28</sup> Different from Hartwig's approach, these systems enabled C–H borylation of cyclopropane chelation assisted by N or O atom. With the assistance of various directing groups, including N-heteroarenes, oximes, imines, and amides, the borylation occurred with remarkable regio- and stereoselectivities. This conversion led to the formation of *cis*-substituted cyclopropyl- and cyclobutylboronates. The successful borylation of sterically congested C–H bonds in substituted cyclopropanes, even including a tertiary C–H bond, showcases the potential of this directed C–H activation strategy for the functionalization of small-ring systems. Furthermore, beyond arylation and trifluoroborate formation, cyclopropylboronate esters can be further converted into primary alcohols through a one-carbon homologation/oxidation sequence.

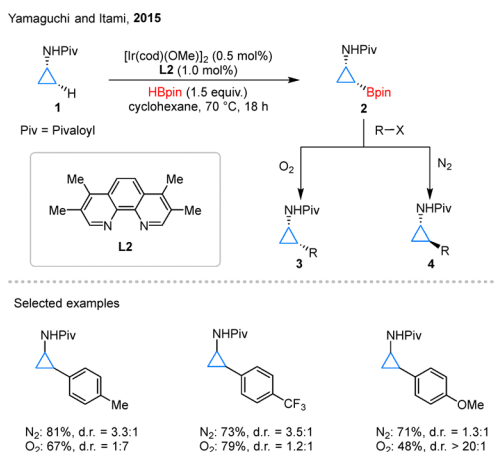
Cyclopropylamines (CPAs) represent a particularly intriguing class of readily accessible cyclopropane derivatives, distinguished by their synthetic versatility.<sup>29</sup> In 2015, Yamaguchi





Scheme 2 Silica-supported catalytic C–H borylation of cyclopropanes.

and Itami pioneered a significant advancement in this field through the development of an Ir-catalyzed, directed C–H borylation of CPAs **1**, employing ligand **L2** to efficiently access cyclopropyl boronate esters **2** (Scheme 3).<sup>30</sup> In the course of reaction optimization, the authors found that the use of **L1** or 4,4'-dtbpy led only to poor outcomes. Switching the ligand to **L2** significantly improved the reactivity, and further adjustments of the boron source and the catalyst/ligand loadings, among other parameters, enabled the identification of the optimal conditions. This methodology enabled subsequent diversification *via* Suzuki–Miyaura coupling reactions, leading to the synthesis of valuable 2-arylcyclopropylamine derivatives. Notably, the stereochemical outcome of this transformation exhibited remarkable sensitivity to atmospheric conditions: under inert nitrogen atmosphere, partial epimerization occurred at the nitrogen center, while oxidative conditions (O<sub>2</sub> atmosphere)



Scheme 3 Iridium-catalyzed C–H borylation of CPAs and the follow-up transformation.

effectively suppressed this process. This atmospheric control allowed for precise access to either *cis*- or *trans*-configured products (**3** or **4**, respectively), providing a unique stereochemical modulation strategy. These findings not only demonstrated the profound influence of reaction conditions on stereoselectivity in cyclopropane functionalization but also underscored the strategic importance of boron chemistry in controlling molecular architecture.

Chiral cyclopropylboronates have garnered increasing attention due to the versatile diversification potential of the C–B bond.<sup>31</sup> In 2017, Yu *et al.* reported a Pd-catalyzed enantioselective C–H borylation reaction using an acetyl-protected aminomethyl oxazoline ligand **L3** (Scheme 4).<sup>32</sup> Using B<sub>2</sub>pin<sub>2</sub> as the boron source, the reaction achieved high enantioselectivity for the borylation of various cyclic amides, including cyclobutanes and cyclohexanes. Notably, subjecting cyclopropanecarboxylic amide **5** to these conditions afforded cyclopropylboronate **6** with excellent enantioselectivity, albeit in 32% yield. The reaction was also accompanied by the formation of the ring-opening byproduct, the geminal diboron compound **7**. This work represented an early foray into the enantioselective C–H borylation of cyclopropanes.

In 2019, Xu and colleagues developed the enantioselective C–H borylation of cyclopropanecarboxamides using iridium catalyst with a chiral bidentate boryl ligand (CBL) **L4** developed by themselves (Scheme 5).<sup>33</sup> Unlike the above palladium catalysis, no ring-opening byproducts were observed in the systems. During reaction optimization, the authors primarily focused on the influence of CBLs on both the yield and enantioselectivity. They found that the steric bulk of the aryl and alkyl substituents on the CBLs was the key factor responsible for the high performance of the reaction. In substrate scope studies, cyclopropanes with imide, alkyl, or aryl substituents were generally compatible with the reaction. Mechanistic studies revealed that ligand **L4** reacts with [Ir(cod)Cl]<sub>2</sub> and B<sub>2</sub>pin<sub>2</sub> to generate a 14-electron Ir(III) complex **10** bearing vacant coordination sites. Upon coordination with substrate **8**, the complex forms intermediate **11**, in which the β-C–H bond is preactivated through an agostic interaction. Subsequent oxidative addition affords Ir(V) species **12**, which then undergoes reductive elimination to deliver the borylated product **9** and intermediate **13**. Finally, **13** reacts with B<sub>2</sub>pin<sub>2</sub> to regenerate **10**. The authors further demonstrated a series of transformations of the boryl cyclopropanes, including Suzuki–Miyaura cross-coupling, alkenylation,



Scheme 4 Asymmetric palladium-catalyzed C–H borylation of cyclopropane.



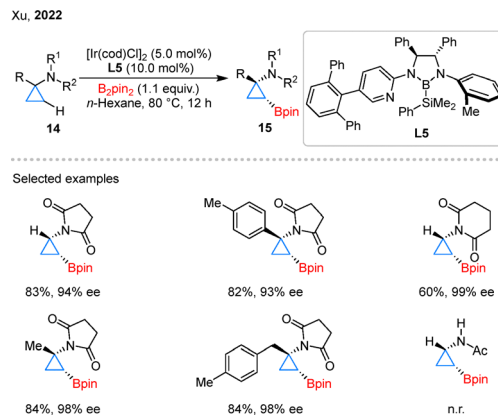


Scheme 5 Asymmetric Ir-catalyzed C–H borylation of cyclopropane-carboxamides.

and carbon homologation/oxidation. Notably, the primary alcohols obtained *via* oxidation could be elaborated through a three-step sequence to afford the antidepressant drug Levomilnacipran.

The versatility of this catalytic system has been further demonstrated through its successful extension to CPAs, enabling the formation of optically active boronates.<sup>34</sup> In 2022, Xu and colleagues achieved the asymmetric borylation of CPAs **14**, marking a notable progression in stereocontrolled cyclopropane functionalization (Scheme 6).<sup>35</sup> By strategically employing succinimide directing groups in conjunction with CBL **L5**, they successfully accessed chiral products **15** with high diaster- and enantio-selectivity. It is noteworthy that the use of acetyl group proved ineffective, highlighting the crucial role of this cyclic directing groups. Mechanistically, the succinimide group serves a dual purpose: it coordinates to the iridium center and modulates the electronic properties of the substrate, thereby facilitating selective  $\beta$ -C–H activation through the formation of a six-membered iridacycle intermediate.

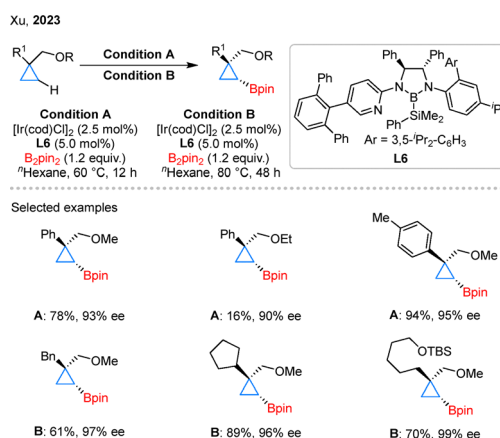
Ether motifs are prevalent in bioactive molecules and synthetic intermediates; however, their weak coordinating ability has traditionally limited their application in asymmetric C–H



Scheme 6 Asymmetric Iridium-catalyzed C–H borylation of CPAs.

activation.<sup>36</sup> In 2023, the Xu group reported an Ir-catalyzed asymmetric C–H borylation of cyclopropanes directed by ether group using CBL **L6** as the ligand (Scheme 7).<sup>37</sup> In substrate scope studies, the MeO group enabled efficient C–H borylation of both aryl- and alkyl-substituted cyclopropanes, whereas the EtO group proved significantly less effective. Notably, alkyl-substituted substrates required higher temperatures and longer reaction times for satisfactory conversion. This result highlights the versatility of CBL-type ligands in C–H borylation, underscoring their remarkable compatibility with diverse directing groups.

Analogous to cyclopropanes, cyclobutanes represent another structurally constrained motif of considerable importance in medicinal chemistry.<sup>38</sup> Indeed, research on the C–H borylation of cyclopropanes and cyclobutanes has often advanced in parallel. As noted above, both Sawamura's and Yu's studies on cyclopropane C–H borylation were accompanied by related investigations on cyclobutanes.<sup>28,32</sup> Furthermore, in 2020, Xu *et al.* employed their developed CBLs to achieve an asymmetric C–H borylation of cyclobutanes.<sup>39</sup> Subsequently, Engle's group extended this concept to the methylenecyclobutanes.<sup>40</sup> In contrast to cyclopropanes, the development of ring-opening borylation of cyclobutanes has been relatively limited, likely



Scheme 7 Asymmetric ether-directed C–H borylation of cyclopropanes.



because the ring strain released upon cleavage of the four-membered ring is much smaller. Recently, inspired by Engle's findings, Lu and Ge achieved ring-opening borylation of methylenecyclobutanes.<sup>41</sup>

### 3. C–C borylation of cyclopropanes

The significant ring-strain inherent in cyclopropanes acts as a strong driving force for ring-opening reactions.<sup>42,43</sup> This property has been extensively exploited as a strategic method in organic synthesis. As a result, cyclopropanes have emerged as highly versatile platforms for selective C–C borylation, enabling the synthesis of a diverse array of regio- and stereodefined organoboron compounds. Given the multitude of C–C activation instances, we have conducted a more meticulous classification of these reactions based on the types of cyclopropanes involved. These cyclopropane derivatives are systematically divided into five categories: (1) alk(en/yn)ylcyclopropanes; (2) *gem*-difluorocyclopropanes; (3) aminocyclopropanes; (4) imino-cyclopropanes; and (5) simple cyclopropanes. The mechanisms of C–C activation typically encompass  $\beta$ -carbon elimination, oxidative addition, and nucleophilic borylation.

#### 3.1. Alk(en/yn)ylcyclopropanes

A wide spectrum of cyclopropanes incorporating unsaturated carbon–carbon bonds has been extensively utilized in C–C borylation reactions, demonstrating remarkable structural diversity. As illustrated in Fig. 5, this includes vinylcyclopropanes (VCPs), benzylidenecyclopropanes (BCPs), vinylidenecyclopropanes, propargylic cyclopropanes, alkylidenecyclopropanes (ACPs), and methylcyclopropanes (MCPs). To facilitate a more systematic and insightful analysis of these transformations, we have implemented a comprehensive classification framework based on reaction patterns. Specifically, these reactions have been categorized into three distinct subgroups: (1) monoborylation, involving the introduction of a single boryl group; (2) diborylation, characterized by the incorporation of two boryl moieties; and (3) borylative functionalization, which encompasses tandem borylation and subsequent functional group transformations.<sup>44</sup>

**3.1.1. Monoborylation.** VCPs represent a unique class of donor–acceptor cyclopropanes that have gained significant attention in synthetic chemistry due to their ability to coordinate with transition metals, facilitating ring-opening reactions and serving as effective substrates for C–C borylation.<sup>45</sup> In a

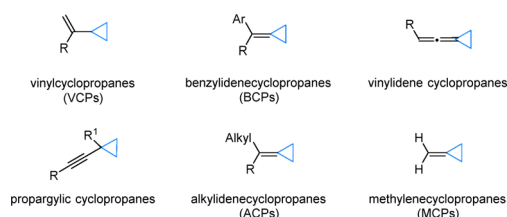


Fig. 5 Structural diversity of cyclopropanes bearing unsaturated C–C bonds.

groundbreaking study, Oshima and Yorimitsu demonstrated a nickel-catalyzed ring-opening borylation of VCPs **16** using  $B_2pin_2$ , which successfully yielded allylboronic esters **17** (Scheme 8).<sup>46</sup> This reaction exhibited remarkable versatility, accommodating a wide range of ester-substituted VCPs. Notably, the steric bulk of the ester group was found to enhance the stereoselectivity of the process. The proposed mechanism begins with the oxidative addition of a Ni(0) species to VCPs **16**, promoted by  $B_2pin_2$ , to form a  $\pi$ -allyl (or oxa- $\pi$ -allyl) nickel intermediate **18**. This intermediate then undergoes transmetalation with a boron enolate species, resulting in the formation of a  $\pi$ -allylnickel complex **19** that incorporates a boron-containing moiety. The subsequent reductive elimination from complex **19** generates the boron enolate, which is then protonated *in situ* to produce the final product **17** and regenerated active Ni complex.

In 2019, Engle *et al.* also developed a copper-catalyzed hydroborylation of BCPs **20**, giving two different products **21** and **22** (Scheme 9).<sup>47</sup> The distinct outcomes observed with different ligands **L7** and **L8**. DFT calculations suggest that the reaction pathway is primarily controlled by the energy difference between two competing steps:  $\beta$ -carbon elimination and protodecupration. Both originate from the same benzylic copper intermediate **23**. The **L7** ligand significantly increases the barrier for  $\beta$ -carbon elimination, while having little effect on protodecupration. As a result, the reaction shifts toward protodecupration, giving cyclopropylboronic ester **21**. In contrast, with the **L8** ligand,  $\beta$ -carbon elimination is more favorable, which aligns with the formation of alkenylboronate **22**.

The introduction of chiral catalysts has enabled the realization of asymmetric hydroborylation of VCPs, marking a stereoselective synthesis. In 2017, Lu and coworkers achieved an advancement in the field by developing an iron-catalyzed hydroborylation of VCPs **24** (Scheme 10).<sup>48</sup> This innovative approach utilized pre-catalyst **25** to efficiently produce homoallylic boronates **26**, achieving high enantiocontrol in the process. In the proposed mechanism, the active Fe–H species



Scheme 8 Nickel-catalyzed ring-opening borylation of VCPs.





Scheme 9 Copper-catalyzed selective hydroborylation of BCPs.



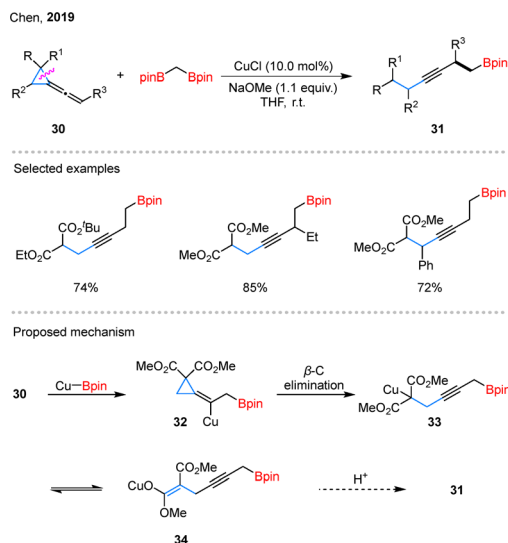
Scheme 10 Asymmetric iron-catalyzed borylation of VCPs.

forms from **25** in the presence of  $\text{NaHBET}_3$ . Subsequent coordination of **24** to complex **25** generates intermediate **27**, which undergoes alkene insertion into the Fe–H bond to afford intermediate **28**. A regioselective  $\beta$ -carbon elimination from **28** produces alkyl iron species **29**, which may undergo  $\beta$ -hydride elimination to give diene byproducts. Finally, ligand exchange between **29** and HBpin regenerates active Fe–H species and releases **26**.

Beyond the well-established VCPs, vinylidene cyclopropanes have emerged as another versatile class of substrates in organic

synthesis.<sup>49</sup> In a notable contribution, Chen and coworkers demonstrated the copper-catalyzed synthesis of homopropargylic boronates **31** using vinylidene cyclopropanes **30** and 1,1-bisborylmethane as starting materials (Scheme 11).<sup>50</sup> This methodology showcased broad substrate compatibility, accommodating vinylidene cyclopropanes with substituents at diverse positions under optimized reaction conditions. In the proposed mechanism, Cu-based carbon nucleophiles undergo migratory insertion with substrate **30** to generate vinyl copper intermediate **32**, which subsequently undergoes  $\beta$ -carbon elimination to form open-chain intermediates (**33** or **34**). These intermediates then react with a proton source to afford functionalized products **31**. Building upon this work, the same research group later reported the selective borylation of vinylidene cyclopropanes using unsymmetrical diboron compounds, further expanding the synthetic utility of this approach.<sup>51</sup>

**3.1.2. Diborylation.** Propargylic cyclopropanes are invaluable reagents in organic synthesis, especially for constructing complex molecules.<sup>52</sup> Based on this substrates, Szabó *et al.* reported a Cu-catalyzed stereo- and regioselective synthesis of alkenyl diboronates **36** and allenyl boronates **37** (Scheme 12).<sup>53</sup> When phosphine **L9** was employed, a range of **36** were obtained with high stereoselectivity. However, substrates bearing more sterically demanding groups required elevated temperatures and prolonged reaction times to achieve good conversions. In contrast, switching the ligand to phosphine **L10** led exclusively to the formation of **37**. In this catalytic system, the Cu catalyst initially forms complex **38** *via* transmetalation with  $\text{B}_2\text{pin}_2$  in the presence of base and either **L9** or **L10**. The complex **38** is selectively inserted into the alkyne moiety of **35** to give **39**. Subsequent ring-opening of the strained cyclopropane in **39** furnishes the allenyl boronate intermediate **40**, which quickly rearranges into the thermodynamically favored product **37**. Notably, the ligand structure critically influences subsequent reaction pathways. With the bulky ligand **L10**, further reaction



Scheme 11 Copper-catalyzed borylative ring-opening of vinylidene cyclopropanes.



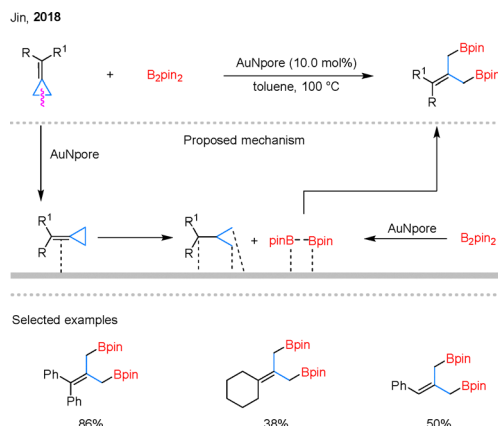


Scheme 12 Copper-catalyzed borylation of propargylic cyclopropanes.

progression stalls at the allenyl stage. However, the less hindered **L9** facilitates further insertion of **L9CuBpin** into **37**, leading to the formation of intermediate **41**, which undergoes  $\gamma$ -protonation to afford product **36**. Thus, ligand choice acts as a strategic ‘switch’, dictating divergent outcomes from a common intermediate.

ACPs and BCPs are known for their heightened ring strain and exhibit distinct reactivity patterns in C–C borylation.<sup>54</sup> In 2018, Jin and colleagues demonstrated that nanoporous gold (AuNPore) could catalyze the diborylation of BCPs or ACPs in a heterogeneous manner, selectively cleaving the distal C–C bond (Scheme 13).<sup>55</sup> Remarkably, this transformation proceeds in the absence of ligands or additives, highlighting the unique surface-mediated reactivity of AuNPore. Beyond its regioselectivity, the catalyst exhibits recyclability and operational stability, underscoring its potential for sustainable and green catalytic applications. However, the substrate scope was largely limited to simple BCPs, while alkyl-substituted analogues generally exhibited lower reactivity and required prolonged reaction times to achieve acceptable yields.

In 2023, Ge and coworkers developed a regiodivergent ring-opening dihydroborylation of BCPs **42** by cobalt catalysis, enabling access to both 1,3- and 1,4-diboronate products **43** and **44** (Scheme 14).<sup>56</sup> Aryl groups with different electronic properties were well tolerated, though bulky substituents required higher temperatures to improve yields. The high regioselectivity is attributed to  $\beta$ -C elimination, which forms



Scheme 13 Nanoporous gold-catalyzed selective diborylation of cyclopropanes.

unique homoallylic cobalt intermediates. In the catalytic cycle,  $\text{Co}(\text{acac})_2$  activated by HBpin and **L** generates  $\text{LCo-H}$ , which inserts into **42** to give benzylcobalt intermediate **45**, followed by  $\beta$ -C elimination to yields homoallylic species **46**. Ligand choice directs the subsequent steps: with rigid **L11**, **46** reacts with HBpin to form **47**, which undergoes  $\sigma$ -bond metathesis to afford 1,4-diboronate **43**, while  $\beta$ -H elimination is suppressed. In contrast, flexible **L12** enables **46** to adopt a coplanar geometry, promoting  $\beta$ -H elimination to generate **48**. Reinsertion of the diene into the Co–H bond generates allylcobalt species **49**, which reacts with HBpin to form **50**. Subsequent Co–H insertion yields **51**, which undergoes  $\sigma$ -bond metathesis with HBpin to give 1,3-diboronate **44** and regenerate the active  $\text{LCo-H}$  catalyst.

In addition, Tu and Peng also developed an Ir-catalyzed 1,*n*-diborylation of cyclopropanes using their newly designed spirocyclic NHC Ir catalyst **53** or **56** (Scheme 15).<sup>57</sup> A range of mono- and diaryl-substituted cyclopropanes **52** or **55** were well tolerated, affording previously rare 1,1-diborylated products **54** or **57**, whereas alkyl-substituted ACPs failed to undergo the transformation. Furthermore, the scope of this diborylation strategy was extended to two additional substrate classes. Specifically, a series of MCPs **58** underwent smooth transformation to deliver the corresponding 1,4-diborylated products **59**. In parallel, cyclopropyl-substituted ACPs **60** were successfully converted into 1,7-diborylated compounds **61** under milder reaction conditions. DFT calculations were performed to investigate the mechanism of the reaction using diaryl-substituted BCPs. The process begins with the form of hemilabile Ir(i) species **62**. This intermediate reacts with  $\text{B}_2\text{pin}_2$  to form the Ir(III) complex **63**. The reductive elimination of **63** affords the Ir(i) species **64**, which undergoes oxidative addition to **52** to yield the cyclic Ir(III) intermediate **65**. Next, a concerted reductive elimination and oxidative addition step converts **65** into the vinyl-Ir(III) complex **66**. A  $\sigma$ -bond metathesis between the Ir–H bond and the phenyl C–B bond then gives **67**. The system undergoes  $\sigma$ -metathesis between the Ir–C bond and the  $\alpha$ -C–H bond of the Bpin group, forming another four-membered Ir(III) complex **68**. This intermediate





Scheme 14 Cobalt-catalyzed diborylation of BCPs.

undergoes intramolecular ligand exchange to form **69**, which subsequently reacts with HBpin to yield **70**. Finally, reductive elimination from **70**, followed by dissociation of the catalyst, furnishes the product **54**.

Enantioselective diborylation has recently emerged as a significant advancement within this topic. A notable contribution by Lu and Ge demonstrated a Cu-catalyzed asymmetric diborylation of BCPs, achieving selective formation of both 1,3- and 1,4-diboronates with chiral bisphosphine ligands **L13** and **L14** (Scheme 16).<sup>58</sup> This methodology efficiently transformed BCPs with various substituents into either 1,4-diboration products **71** or 1,3-diboration products **72** with excellent enantioselectivity. Mechanistic studies suggest that the reaction begins with LCu-H insertion into BCPs to form benzyl copper species **73**, which undergoes  $\beta$ -carbon elimination to give homoallylic cuprate **74**.  $\sigma$ -Bond metathesis with HBpin generates a *Z/E* mixture of **75** and regenerates LCu-H. In the 1,4-pathway, (*E*)-**75** inserts into Cu-H to form **76**, leading to product **71**. In contrast, (*E*)-**75** inserts into LCu-Bpin yields **77**, which affords 1,3-diboronate **72**.

**3.1.3. Borylative functionalization.** Silylboranes have gained significant attention in organic synthesis due to their ability to selectively functionalize both the silicon and boron centers.<sup>59</sup> In 2000, Suginome and Ito disclosed a silaborylation of ACPs enabled by Pd or Pt catalysis, achieving regio- and

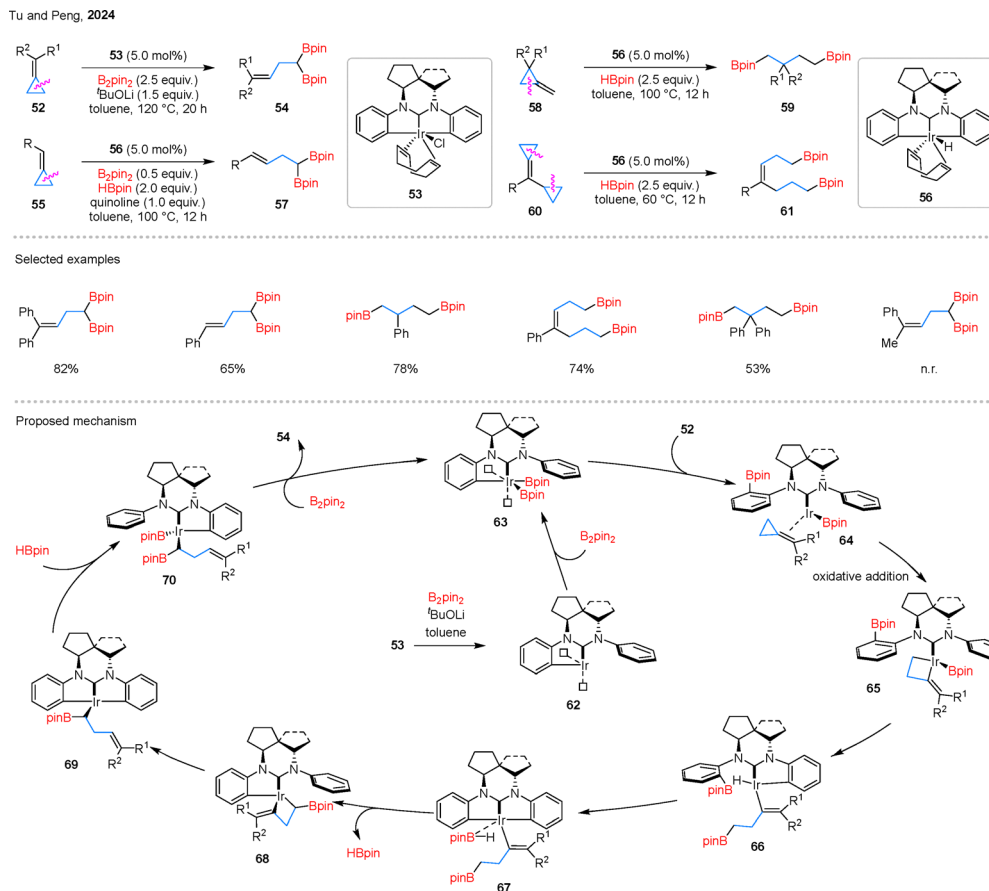
stereoselective C–C bond cleavage. (Scheme 17).<sup>60</sup> The reaction outcome was strongly influenced by the electronic and steric nature of the substituents. Substrates **78** bearing phenyl or ester groups predominantly underwent cleavage of the proximal C–C bond *trans* to the substituent, leading to *Z*-configured products **79**. In contrast, ACPs **80** exhibited more flexible reactivity, where the regioselectivity was governed by the metal catalyst. A Pt catalyst favored cleavage at the proximal bond to form **81**, whereas a Pd catalyst facilitated distal bond scission to afford **82**. The proposed mechanism for forming **79** typically involves C=C migratory insertion followed by  $\beta$ -carbon elimination to yield homoallylic intermediates **83**. However, this pathway fails to explain the high *Z*-selectivity observed in Pt-catalyzed reactions with various substrates. An alternative mechanism involving oxidative addition of the proximal C–C bond may better account for this selectivity, as the electronic nature of substituents can influence the cleavage site. This pathway is likely favored when steric or electronic factors hinder migratory insertion. A similar oxidative addition may also apply to distal C–C bond cleavage, forming product **82**.

In 2007, the same research group successfully developed an asymmetric variant of the silaborylation of MCPs, employing palladium catalysis in conjunction with chiral ligand **L15** to yield enantioenriched products (Scheme 18A).<sup>61</sup> The reaction demonstrated excellent efficiency with bicyclic MCPs, consistently delivering the desired products. However, substrates lacking ring fusion or those containing cyclic acetal motifs exhibited reduced enantioselectivities and yields. The use of polymer-supported chiral ligands offers significant advantages, including ease of recovery and potential for reuse.<sup>62</sup> Building on this concept, the group further explored Pd-catalyzed asymmetric silaborylation of MCPs utilizing a helically chiral polymeric ligand **L16** (Scheme 18B).<sup>63</sup> Remarkably, the application of **L16** consistently provided higher enantioselectivity compared to previously reported systems. This enhancement is attributed to the polymeric ligand's ability to create a long-range chiral environment around the palladium center. In contrast to conventional small-molecule ligands, this unique feature not only improves catalytic reactivity but also enhances stereocontrol, offering a more efficient and sustainable approach to asymmetric synthesis.

The borylative functionalization of cyclopropanes is not limited to silaborylation. In 2022, Peng and coworkers reported a Cu-catalyzed borylacylation of BCPs that proceeds through proximal C–C bond cleavage, delivering 1,3-borylacylated products (Scheme 19).<sup>64</sup> Aryl- and naphthyl-substituted BCPs, along with a variety of chloroformate electrophiles, reacted efficiently under the standard conditions. Using cyclopropyl-substituted BCPs, the same group further developed a regioselective 1,5-borylacylation using a Cu/Pd dual-catalytic system.<sup>65</sup>

The substrate scope of alkene borocarbonylation has been largely limited to styrene derivatives,<sup>66</sup> whereas BCPs, as a distinct alkene analogue, have shown potential as viable substrates for such transformations. In 2022, Wu and colleagues established a Cu/Pd dual-catalytic regiodivergent borylacylation of BCPs with aryl iodides and CO (Scheme 20).<sup>67</sup> By carefully





Scheme 15 Iridium-catalyzed regioselective 1,*n*-diborylation of cyclopropanes.

tuning the metal combination and ligand **L11**, the reaction of BCPs could be steered to furnish either  $\gamma$ -vinylboryl ketones **84** or  $\beta$ -cyclopropylboryl ketones **85**. Under the standard conditions, the protocol exhibited broad substrate compatibility, tolerating BCPs bearing aryl or heteroaryl groups as well as various aryl iodides. The reaction showcases precise regioselectivity control enabled by tailored metal–ligand combinations, underscoring its unique mechanistic design.

The development of asymmetric borylacylation has emerged as a powerful strategy for accessing enantiomerically enriched aminoboronates, marking a significant advancement in catalytic methodology.<sup>68</sup> In a pioneering contribution, Su and colleagues reported a Cu-catalyzed 1,4-borylamination of BCPs through a cascade sequence involving hydroborylation followed by hydroamination (Scheme 21).<sup>69</sup> This method demonstrated broad substrate tolerance, accommodating BCPs, as well as various aminating reagents. Mechanistic studies revealed that the transformation proceeds *via* two interconnected catalytic cycles. In the hydroborylation cycle, **L17Cu–H** inserts into BCPs to form benzyl copper intermediate **87**, which undergoes  $\beta$ -carbon elimination and  $\sigma$ -bond metathesis to generate borylated intermediate **88**. In the subsequent hydroamination cycle, **88** undergoes regio- and enantioselective hydrogenation to form intermediate **89**, which then reacts with a hydroxylamine ester to yield the 1,4-borylaminated product **86**. Later, Wu and

coworkers further advanced the field by reporting a Cu-catalyzed borylation of BCPs, enabling the synthesis of both chiral 1,4-borylamine and 1,4-borylcarboxamidation products.<sup>70</sup>

### 3.2. Gem-difluorocyclopropanes

Monofluoroalkenes are valuable fluorinated motifs often employed in medicinal chemistry as a metabolically stable bioisostere for amide functionalities ( $-\text{NH}-\text{CO}-$ ).<sup>71</sup> In 2021, Fu and Gong reported a Cu/Pd-cocatalyzed three-component coupling of *gem*-difluorocyclopropane **90** with alkynes and  $\text{B}_2\text{pin}_2$ , producing monofluorinated alkenes **92** (Scheme 22).<sup>72</sup> Using an pre-catalyst **91**, internal and terminal alkynes, as well as aryl-substituted *gem*-difluorocyclopropanes, were effectively converted into the desired products. Notably, natural products such as coumarin were also amenable to late-stage functionalization under the standard conditions. In the proposed mechanism, the reaction begins with borylcupration of the alkyne, generating a  $\beta$ -borylalkenyl copper species **93**. Concurrently, the Pd(0) catalyst activates **90** *via* C–C bond cleavage accompanied by C–F bond activation, forming an allyl–Pd(II) complex **94**. Subsequent transmetalation between intermediates **93** and **94** produces a Pd(II) species **95**, which undergoes reductive elimination to deliver the target product **92**.



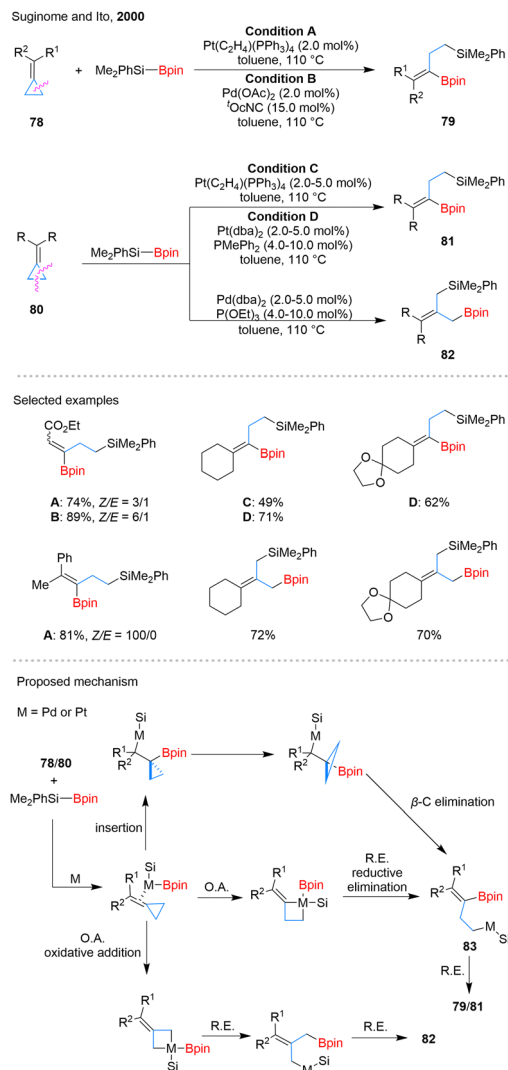


Scheme 16 Copper-catalyzed asymmetric diborylation of BCPs.

Expanding their catalytic repertoire, the research team also uncovered *t* borylfluoroallylation of alkenes using dual Cu/Pd-catalysis. This transformation, which employs *gem*-difluorocyclopropanes and  $B_2pin_2$  as key reagents, efficiently delivers monofluoroalkene scaffolds **96** with high precision (Scheme 23A).<sup>73</sup> The reaction demonstrated broad compatibility with a range of substituted *gem*-difluorinated cyclopropanes and alkenes, showcasing its synthetic versatility. Notably, rather than isolating the boronate intermediates, the authors opted for their direct oxidation to the corresponding alcohols, streamlining the synthetic process. Building upon this success, they further developed the Pd-catalyzed coupling of *gem*-difluorocyclopropanes with *gem*-diborylalkanes **97**, yielding boryl-substituted fluorinated alkenes **98** with excellent control over regioselectivity (Scheme 23B).<sup>74</sup> The reaction exhibited remarkable tolerance to variations in the electronic properties of substituents. However, it was observed that more sterically demanding substrates, such as 1,2-disubstituted *gem*-difluorocyclopropanes, remained incompatible with the optimized reaction conditions.

### 3.3. Aminocyclopropanes

The nitrogen substituent in cyclopropanes can act as an internal driving force to facilitate C–C bond cleavage of the strained ring.<sup>5</sup> In, 2021, Shi *et al.* disclosed a Rh-catalyzed proximal-selective C–C bond activation of NHPiv-substituted CPAs **99**, affording  $\gamma$ -amino boronates **100** (Scheme 24).<sup>75</sup> Substrate scope investigations showed that both alkyl and aryl groups

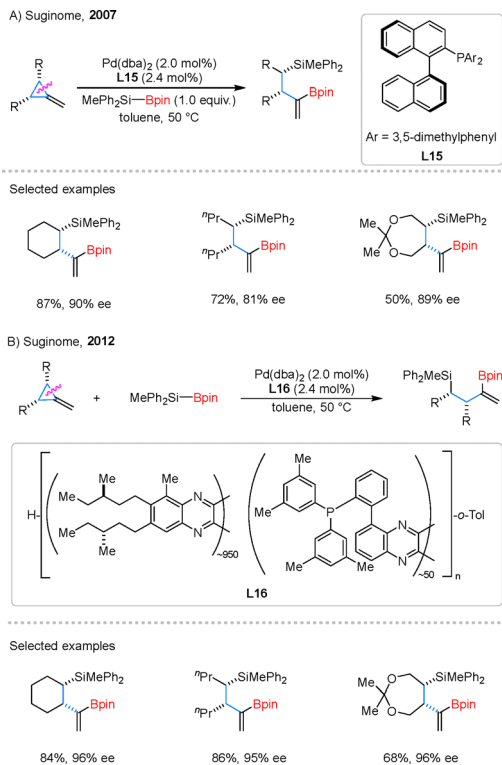


Scheme 17 Catalytic silaborylation of ACPs.

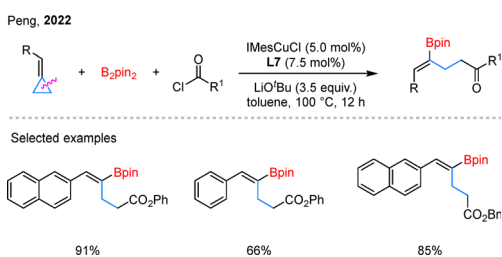
at the R position were well tolerated. In contrast, substrates with substituents at the R<sup>1</sup> position required higher catalyst and ligand loadings, as well as extended reaction times, to achieve satisfactory results. In the proposed mechanism, the reaction is initiated with ligand exchange between the cyclooctadiene (cod) ligand in complex **101** and substrate **99**, affording intermediate **102**. Chelation assisted by the amide oxygen, proximal C–C bond cleavage then occurs in **102** to generate intermediate **103**. Intermediate **104** is subsequently formed through the reaction of **103** with HBpin. Computational analysis revealed that the hydroborylation step likely follows a  $\sigma$ -complex-assisted metathesis ( $\sigma$ -CAM) pathway rather than oxidative addition. From intermediate **104**, re-coordination of the cod ligand affords intermediate **105**, which undergoes reductive elimination of the C–H bond to deliver the product-coordinated **106**.

Subsequently, Shi and colleagues further developed an enantioselective asymmetric hydroborylation of CPAs **107**, affording chiral aminoboronates **108** (Scheme 25).<sup>76</sup> The key





Scheme 18 Palladium-catalyzed asymmetric silaborylation of MCPs.



Scheme 19 Copper-catalyzed borylacylation of BCPs.



Scheme 20 Catalytic regiodivergent borylacylation of BCPs.



Scheme 21 Copper-catalyzed asymmetric borylmination of BCPs.

Scheme 22 Catalytic *cis*-borylfluoroallylation of alkynes.

to the high enantioselectivity is the combination of the chiral phosphite **L18** and the anionic acac ligand with rhodium catalyst. The reaction system shows good tolerance towards

aryl substituents with different electronic effects on the cyclopropane ring. However, when alkyl groups are present, the enantioselectivities are significantly lower. Mechanistic studies



Scheme 23 Catalytic borylation of *gem*-difluorinated cyclopropanes.

Scheme 24 Rhodium-catalyzed proximal-selective C–C borylation of CPAs.

suggest that the active catalytic species **109**, generated from cyclopropane **107**, **L18**, and the Rh-bound acac ligand, undergoes proximal-selective C–C bond oxidative addition to form rhodacycle **110**. Ligand exchange with HBpin produces intermediate **111**, which undergoes  $\sigma$ -CAM to generate **112**. Reductive elimination from **112** *via* transition state **113** yields product

**108** and regenerates catalyst **109** through ligand exchange with **107**.

In addition to rhodium catalysis, the same conversion can be achieved by inexpensive and earth-abundant group IV metals. In 2024, Wu and colleagues reported the example of zirconium-catalyzed hydroborylation of CPAs **114** (Scheme 26).<sup>77</sup> Notably, hafnium also exhibited comparable catalytic efficiency for this transformation. Within the substrate scope, aryl-, alkyl-, and amide-substituted cyclopropanes were well tolerated. However, for 1,2-disubstituted cyclopropane substrates, the system exhibited limited diastereocontrol. Mechanistically, *in situ* generated Zr–H reacts with N–H bonds of **114** to form N–Zr species **116** with H<sub>2</sub> release.  $\beta$ -Carbon elimination then cleaves the C–C bond, yielding zirconium species **117**. Subsequently, **117** undergoes C–Zr and H–B bond metathesis with HBpin, producing intermediate **118** and regenerating the Zr–H species. In the second catalytic cycle, hydride transfer from Zr–H to intermediate **118** forms intermediate **119**, which is further reduced by the previously released H<sub>2</sub> to generate **115**.

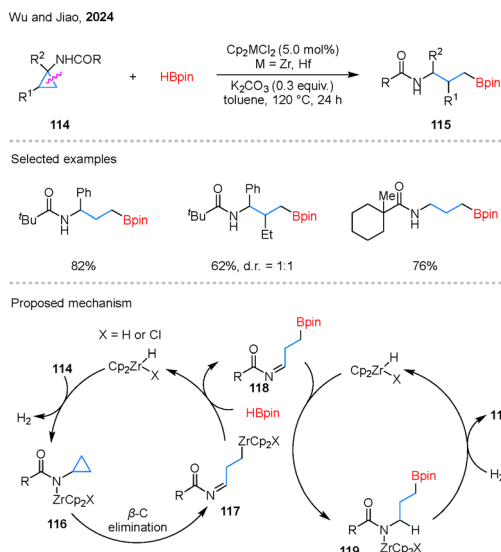
Notably, Wu and colleagues recently discovered that the above hydroboration can proceed under a meta-free approach just using HBcat (Scheme 27).<sup>78</sup> This method exhibits broad substrate compatibility, particularly in the late-stage modification of pharmaceutical compounds such as ibuprofen. However, substrates bearing carboxylic acids on the aryl ring showed poor reactivity. Mechanistic insights from DFT calculations indicate that the transformation begins with the formation of a van der Waals complex **120** between HBcat and the cyclopropane substrate. The approach of HBcat toward the less hindered C–C bond proceeds through a ring-opening transition state **121**, which serves as the rate-determining step and leads to **122** stabilized by coordination with the oxygen atom of HBcat. A subsequent hydride transfer from the boron center to the adjacent carbocation *via* **123** furnishes the borylated product **124**.

Beyond the above hydroborylation strategies, a novel  $\sigma$ -C–C bond eliminative borylation of cyclopropanes has emerged as a powerful synthetic tool. In a significant contribution, Shi and coworkers introduced a stereoselective C–C bond activation of CPAs **125** mediated by BCl<sub>3</sub>, which enables the synthesis of  $\gamma$ -borylenamides **126** under metal-free conditions (Scheme 28).<sup>79</sup> Notably, this stereoconvergent protocol is highly remarkable as it can tolerate *cis/trans* mixtures of substrates and produces products with high stereoselectivity. Under the optimized reaction conditions, a wide range of alkyl- and aryl-substituted substrates, including 1,2-disubstituted cyclopropanes, can successfully yield the desired products. However, substrates containing alkyne groups are not compatible with this reaction system. According to the proposed mechanism, substrate **125** first coordinates with BCl<sub>3</sub> to form intermediate **127**, where intramolecular O–B coordination enhances the acidity of the adjacent N–H bond, facilitating deprotonation by the CHMP *via* transition state **128**. The resulting species **129** undergoes halide abstraction by BCl<sub>3</sub> through transition state **130** to generate imine intermediate **131**. Guided by the Piv group, **131** inserts regioselectively into the C–C bond to form intermediate **132**.





Scheme 25 Asymmetric rhodium-catalyzed hydroboration of CPAs.



Scheme 26 Catalyzed hydroboration of CPAs by earth-abundant group IV metals.

Subsequent deprotonation leads to **133**, and a final rearrangement and proton dissociation affords product **134**.

### 3.4. Iminocyclopropanes

1,2-Azaborines are aromatic BN heterocycles considered as benzene isosteres, and their increased polarity and altered electronic properties have been associated with enhanced solubility and biological performance—features that have inspired growing interest in their synthetic development.<sup>80</sup> In



Scheme 27 Metal-free hydroborylation of CPAs.

2023, Dong, Liu, and Houk have illuminated that cyclopropane adorned with electron-withdrawing moieties, such as imines, possess the capacity to undergo nucleophilic eliminative ring fission with the aid of a boron electrophile and a Lewis catalyst (Scheme 29).<sup>81</sup> Aromatic and aliphatic amines were both well



Scheme 28 Stereoconvergent  $\sigma$ -C–C bond eliminative borylation of cyclopropanes.

tolerated under the reaction conditions, and dibromoboranes bearing aryl or alkyl substituents proved to be suitable coupling partners. Moreover, substrates derived from drug molecules

such as ibuprofen also participated smoothly in the reaction, although a few examples showed relatively low yields. In the proposed mechanism, **135** undergoes boron-mediated C–C bond cleavage to generate **137**, which then undergoes reductive elimination to afford diene **138**. DFT calculations suggest that diene *s-trans*-**138** preferentially undergoes a  $6\pi$ -electrocyclization *via* transition state **139** to form the cyclic *N*-borylimine **140**. This intermediate then undergoes DBU-mediated elimination of HBr to furnish the pyridine borane product **136**.



Scheme 29 Borylative ring-opening of cyclopropyl imines or ketones.

### 3.5. Simple cyclopropanes

Although simple cyclopropanes are among the most prevalent three-membered ring motifs, methods for their selective ring-opening and borylation remain limited.<sup>82</sup> In 2010, Stephan and colleagues disclosed the ring-opening of nonactivated cyclopropanes using frustrated Lewis pairs comprising phosphine and  $B(C_6F_5)_3$ , exemplified by the direct electrophilic attack of  $B(C_6F_5)_3$  on cyclopropylbenzene to generate zwitterionic phosphonium borates (Scheme 30).<sup>83</sup>

In 2018, Shi and Houk pioneered a metal-free  $\sigma$ -bond hydroboration of nonactivated cyclopropanes, employing  $BBr_3$  as a Lewis acid catalyst and  $PhSiH_3$  as the hydride donor (Scheme 31).<sup>84</sup> This innovative methodology exhibits anti-Markovnikov selectivity, mirroring the classical Brown hydroboration. The optimized protocol demonstrates exceptional versatility, facilitating the efficient transformation of diverse cyclopropane derivatives, including spiro, aryl, and alkyl-

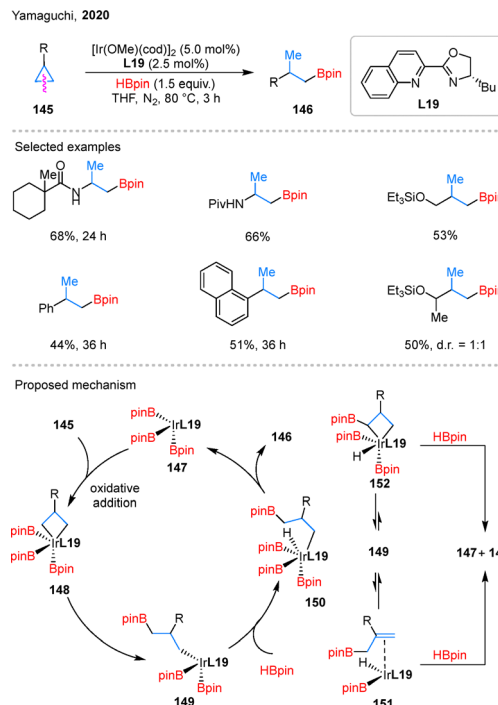
Scheme 30 Borylation ring-opening of nonactivated cyclopropanes with  $B(C_6F_5)_3$ .



**Scheme 31** Borylation ring-opening of nonactivated cyclopropanes with BBr<sub>3</sub>.

substituted variants, into their corresponding borylated products. Notably, the system's robustness was further highlighted by the successful 1,3-hydroboration of cyclopropane gas under balloon pressure, yielding <sup>10</sup>PrBpin in an impressive 71% yield. Comprehensive mechanistic investigations, supported by DFT calculations, have unveiled a sophisticated reaction pathway. The transformation initiates with the electrophilic activation of cyclopropanes **141** by BBr<sub>3</sub>, generating reactive intermediate **142**. This key species subsequently undergoes hydride abstraction from PhSiH<sub>3</sub> through a well-defined transition state **143**, ultimately delivering the borylated product **144**.

In addition, transition-metal catalysis can also facilitate the hydroborylation of simple cyclopropanes. In 2020, Yamaguchi and coworkers reported an Ir-catalyzed distal-selective hydroborylation of cyclopropanes **145** (Scheme 32).<sup>85</sup> Remarkably, this reaction does not require any directing groups and results in the formation of alkylboronates **146**. The reaction accommodates amino, aryl, and silyl ether substituents on the cyclopropane ring, which broadens its applicability in organic synthesis. Mechanistically, a five-coordinate Ir complex **147** serves as the catalytically active species. In the presence of **L19**, oxidative addition of the Cβ–Cγ bond in **145** to complex **147** forms intermediate **148**, which undergoes reductive elimination to give complex **149**. From this point, three downstream pathways are proposed, interconverting through equilibria between intermediates **150**, **151**, and **152**. Among these, the pathway proceeding *via* **150** is the most favorable and ultimately furnishes the hydroborylated product **146**. However, despite the use of the chiral ligand **L19**, enantioselectivity was not induced in this reaction.



**Scheme 32** Iridium-catalyzed distal C–C borylation of cyclopropanes.

## 4. Conclusions and perspectives

Over the past two decades, the cyclopropane-to-organoboron conversion has witnessed transformative progress, driven primarily by innovative strategies for C–H and C–C bond activation. This evolution has unlocked access to structurally complex and diverse boron-containing architectures from readily functionalized cyclopropanes, leveraging both catalyst-free and catalytic approaches. These advancements establish robust synthetic platforms with significant potential for rapid molecular construction.

Despite these remarkable achievements, pivotal challenges remain that define the future trajectory of this dynamic field: (a) examples on C–H borylation of cyclopropanes remains significantly underdeveloped compared to C–C activation. Furthermore, current reliance on directing groups (*e.g.*, amides, ethers) enables enantioselectivity but suffers from limited directing group diversity and a narrow scope of catalyst types. A fundamental frontier lies in achieving directing-group-independent asymmetric C–H borylation of simple, unactivated cyclopropanes. Overcoming this requires pioneering catalyst design (*e.g.*, novel chiral ligands, earth-abundant metal complexes) and a deeper mechanistic understanding of stereoinduction in the absence of inherent directing effects. (b) Asymmetric C–C borylation strategies are currently restricted primarily to vinylcyclopropanes, proceeding *via* metal-boryl insertion followed by β-hydride elimination. While our group recently expanded this scope through the first directing-group-assisted asymmetric C–C borylation of cyclopropanes, such examples are exceedingly rare. The development of broadly applicable, catalytic methodologies for asymmetric C–C



borylation across diverse cyclopropane scaffolds (*e.g.*, alkyl-, aryl-, heteroatom-substituted) represents an imperative and fertile area for exploration. This necessitates exploring alternative activation modes beyond classical activation pathways. (c) The utilization of simple cyclopropanes lacking strong electronic biases or directing functionalities presents a formidable challenge. Achieving regio- and stereoselective borylation in these substrates demands innovative strategies to override inherent electronic and steric similarities. Research must focus on exploiting subtle conformational preferences, designing highly selective catalysts, or employing transient directing groups to impart the necessary control. (d) Current methodologies predominantly operate *via* conventional two-electron reaction manifolds. Integrating external fields—particularly photochemical and electrochemical activation—promises to revolutionize this chemistry. Such approaches could unlock radical-based mechanisms, single-electron transfer pathways, or redox-neutral processes, significantly broadening the reaction scope, enhancing functional group tolerance, and enabling novel disconnection strategies inaccessible *via* thermal routes. (e) Translating these sophisticated methodologies into practical industrial processes remains limited. Key hurdles include cost efficiency (catalyst loading, ligand cost, boron source), operational simplicity (reaction setup, workup), scalability, and environmental sustainability (solvent choice, waste generation). Although metal-free borylation offers advantages in yield and speed, the development of scalable, continuous-flow technologies and integration with downstream functionalization are critical priorities to accelerate the discovery and production of pharmaceuticals and bioactive molecules.

This review has chronicled the remarkable progress and persistent challenges in cyclopropane-to-organoboron conversion. We envision this field evolving into a versatile and transformative paradigm for synthetic organic chemistry. Addressing the outlined challenges will not only advance fundamental boron and cyclopropane chemistry but also foster the discovery of novel bioactive agents and functional materials. We anticipate that multidisciplinary collaborations—spanning catalysis, mechanistic studies, computational design, and process chemistry—will be essential to unlock the full potential of this powerful synthetic strategy. It is our sincere hope that this perspective serves as a catalyst, inspiring continued innovation and exploration in this exciting domain.

## Conflicts of interest

The authors declare no competing financial interest.

## Data availability

No primary research results, software or code has been included and no new data were generated or analysed as part of this review.

## Acknowledgements

We would like to thank Financial support from the National Key R&D Program of China (2022YFA1503200), the National Natural Science Foundation of China (Grants 2024101703, 22025104, 22171134, and 21972064), the Jiangsu Funding Program for Excellent Postdoctoral Talent (Grant 2025ZB263), and the Fundamental Research Funds for the Central Universities (Grant 020514380326) for their financial support.

## References

- 1 C. Ebner and E. M. Carreira, *Chem. Rev.*, 2017, **117**, 11651–11679.
- 2 A. L. Gabbey, K. Scotchburn and S. A. L. Rousseaux, *Nat. Rev. Chem.*, 2023, **7**, 548–560.
- 3 A. U. Augustin and D. B. Werz, *Acc. Chem. Res.*, 2021, **54**, 1528–1541.
- 4 M.-M. Wang, T. V. T. Nguyen and J. Waser, *Chem. Soc. Rev.*, 2022, **51**, 7344–7357.
- 5 O. O. Sokolova and J. F. Bower, *Chem. Rev.*, 2021, **121**, 80–109.
- 6 Y. Cohen, A. Cohen and I. Marek, *Chem. Rev.*, 2021, **121**, 140–161.
- 7 D. Nam, V. Steck, R. J. Potenzino and R. Fasan, *J. Am. Chem. Soc.*, 2021, **143**, 2221–2231.
- 8 H. E. Simmons and R. D. Smith, *J. Am. Chem. Soc.*, 1958, **80**, 5323–5324.
- 9 V. A. Petrov and W. Marshall, *J. Fluorine Chem.*, 2012, **133**, 61–66.
- 10 E. J. Corey and M. Chaykovsky, *J. Am. Chem. Soc.*, 1965, **87**, 1353–1364.
- 11 X. Bugaut, F. Liu and F. Glorius, *J. Am. Chem. Soc.*, 2011, **133**, 8130–8133.
- 12 A. N. Baumann, F. Schüppel, M. Eisold, A. Kreppel, R. de Vivie-Riedle and D. Didier, *J. Org. Chem.*, 2018, **83**, 4905–4921.
- 13 C. Andersen, V. Ferey, M. Dumas, P. Bernardelli, A. Guérinot and J. Cossy, *Org. Lett.*, 2019, **21**, 2285–2289.
- 14 B. M. Coleridge, C. S. Bello and A. Leitner, *Tetrahedron Lett.*, 2009, **50**, 4475–4477.
- 15 E. J. Corey, S. A. Rao and M. C. Noe, *J. Am. Chem. Soc.*, 1994, **116**, 9345–9346.
- 16 A. J. J. Lennox and G. C. Lloyd-Jones, *Chem. Soc. Rev.*, 2014, **43**, 412–443.
- 17 R. J. Grams, W. L. Santos, I. R. Scorei, A. Abad-García, C. A. Rosenblum, A. Bitá, H. Cerecetto, C. Viñas and M. A. Soriano-Ursúa, *Chem. Rev.*, 2024, **124**, 2441–2511.
- 18 T. Ishiyama, N. Matsuda, N. Miyaoura and A. Suzuki, *J. Am. Chem. Soc.*, 1993, **115**, 11018–11019.
- 19 I. F. Yu, J. W. Wilson and J. F. Hartwig, *Chem. Rev.*, 2023, **123**, 11619–11663.
- 20 S. J. Geier, C. M. Vogels, J. A. Melanson and S. A. Westcott, *Chem. Soc. Rev.*, 2022, **51**, 8877–8922.
- 21 B. Zhao, Z. Li, Y. Wu, Y. Wang, J. Qian, Y. Yuan and Z. Shi, *Angew. Chem., Int. Ed.*, 2019, **58**, 9448–9452.



- 22 M. Shimizu, M. Schelper, I. Nagao, K. Shimono, T. Kurahashi and T. Hiyama, *Chem. Lett.*, 2006, **35**, 1222–1223.
- 23 A. De Meijere, *Angew. Chem., Int. Ed. Engl.*, 1979, **18**, 809–826.
- 24 S. J. Blanksby and G. B. Ellison, *Acc. Chem. Res.*, 2003, **36**, 255–263.
- 25 S. Löhr and A. de Meijere, *Synlett*, 2001, 0489–0492.
- 26 R. Bisht, C. Haldar, M. M. M. Hassan, M. E. Hoque, J. Chaturvedi and B. Chattopadhyay, *Chem. Soc. Rev.*, 2022, **51**, 5042–5100.
- 27 C. W. Liskey and J. F. Hartwig, *J. Am. Chem. Soc.*, 2013, **135**, 3375–3378.
- 28 R. Murakami, K. Tsunoda, T. Iwai and M. Sawamura, *Chem. – Eur. J.*, 2014, **20**, 13127–13131.
- 29 P. Bertus and J. Caillé, *Chem. Rev.*, 2025, **125**, 3242–3377.
- 30 S. Miyamura, M. Araki, T. Suzuki, K. Itami and J. Yamaguchi, *Angew. Chem., Int. Ed.*, 2015, **54**, 846–851.
- 31 D. Y.-K. Chen, R. H. Pouwer and J.-A. Richard, *Chem. Soc. Rev.*, 2012, **41**, 4631.
- 32 J. He, Q. Shao, Q. Wu and J.-Q. Yu, *J. Am. Chem. Soc.*, 2017, **139**, 3344–3347.
- 33 Y. Shi, Q. Gao and S. Xu, *J. Am. Chem. Soc.*, 2019, **141**, 10599–10604.
- 34 T. T. Talele, *J. Med. Chem.*, 2016, **59**, 8712–8756.
- 35 Y. Shi, Y. Yang and S. Xu, *Angew. Chem., Int. Ed.*, 2022, **61**, e202201463.
- 36 K. M. Engle, T.-S. Mei, M. Wasa and J.-Q. Yu, *Acc. Chem. Res.*, 2012, **45**, 788–802.
- 37 T. Xie, L. Chen, Z. Shen and S. Xu, *Angew. Chem., Int. Ed.*, 2023, **62**, e202300199.
- 38 E. Lee-Ruff and G. Mladenova, *Chem. Rev.*, 2003, **103**, 1449–1484.
- 39 X. Chen, L. Chen, H. Zhao, Q. Gao, Z. Shen and S. Xu, *Chin. J. Chem.*, 2020, **38**, 1533–1537.
- 40 T. Kang, T. G. Erbay, K. L. Xu, G. M. Gallego, A. Burtea, S. K. Nair, R. L. Patman, R. Zhou, S. C. Sutton, I. J. McAlpine, P. Liu and K. M. Engle, *ACS Catal.*, 2020, **10**, 13075–13083.
- 41 W. Zheng, Y. Cao, B. B. Tan, Y. Wang, S. Ge and Y. Lu, *J. Am. Chem. Soc.*, 2025, **147**, 12273–12284.
- 42 A. de Meijere, *Chem. Rev.*, 2003, **103**, 931–932.
- 43 M. Wang and Z. Shi, *Chem. Rev.*, 2020, **120**, 7348–7398.
- 44 Y. Zhu, J. Li, H. Zhao and B. Su, *Chin. J. Chem.*, 2024, **42**, 3588–3604.
- 45 V. Pirenne, B. Muriel and J. Waser, *Chem. Rev.*, 2021, **121**, 227–263.
- 46 K. Oshima, Y. Sumida and H. Yorimitsu, *Org. Lett.*, 2008, **10**, 4677–4679.
- 47 J. M. Medina, T. Kang, T. G. Erbay, H. Shao, G. M. Gallego, S. Yang, M. Tran-Dubé, P. F. Richardson, J. Derosa, R. T. Helsel, R. L. Patman, F. Wang, C. P. Ashcroft, J. F. Braganza, I. McAlpine, P. Liu and K. M. Engle, *ACS Catal.*, 2019, **9**, 11130–11136.
- 48 C. Chen, X. Shen, J. Chen, X. Hong and Z. Lu, *Org. Lett.*, 2017, **19**, 5422–5425.
- 49 M. Shi, L.-X. Shao, J.-M. Lu, Y. Wei, K. Mizuno and H. Maeda, *Chem. Rev.*, 2010, **110**, 5883–5913.
- 50 J. Chen, S. Gao and M. Chen, *Chem. Sci.*, 2019, **10**, 10601–10606.
- 51 J. Chen, S. Gao and M. Chen, *Org. Lett.*, 2019, **21**, 8800–8804.
- 52 M. Rubin, M. Rubina and V. Gevorgyan, *Chem. Rev.*, 2007, **107**, 3117–3179.
- 53 J. Zhao and K. J. Szabó, *Angew. Chem., Int. Ed.*, 2016, **55**, 1502–1506.
- 54 A. Brandi, S. Cicchi, F. M. Cordero and A. Goti, *Chem. Rev.*, 2014, **114**, 7317–7420.
- 55 Q. Chen, X. Zhang, S. Su, Z. Xu, N. Li, Y. Li, H. Zhou, M. Bao, Y. Yamamoto and T. Jin, *ACS Catal.*, 2018, **8**, 5901–5906.
- 56 B. B. Tan, M. Hu and S. Ge, *Angew. Chem., Int. Ed.*, 2023, **62**, e202307176.
- 57 W.-F. Wang, K. Lu, P.-R. Liu, H.-H. Zeng, L.-M. Yang, A.-J. Ma, Y.-Q. Tu and J.-B. Peng, *ACS Catal.*, 2024, **14**, 5156–5166.
- 58 W. Zheng, B. B. Tan, S. Ge and Y. Lu, *J. Am. Chem. Soc.*, 2024, **146**, 5366–5374.
- 59 M. Oestreich, E. Hartmann and M. Mewald, *Chem. Rev.*, 2013, **113**, 402–441.
- 60 M. Suginome, T. Matsuda and Y. Ito, *J. Am. Chem. Soc.*, 2000, **122**, 11015–11016.
- 61 T. Ohmura, H. Taniguchi, Y. Kondo and M. Suginome, *J. Am. Chem. Soc.*, 2007, **129**, 3518–3519.
- 62 J. Lu and P. H. Toy, *Chem. Rev.*, 2009, **109**, 815–838.
- 63 Y. Akai, T. Yamamoto, Y. Nagata, T. Ohmura and M. Suginome, *J. Am. Chem. Soc.*, 2012, **134**, 11092–11095.
- 64 L.-M. Yang, H.-H. Zeng, X.-L. Liu, A.-J. Ma and J.-B. Peng, *Chem. Sci.*, 2022, **13**, 7304–7309.
- 65 H.-H. Zeng, Y.-Q. Wang, Y.-Y. He, X.-L. Zhong, H. Li, A.-J. Ma and J.-B. Peng, *J. Org. Chem.*, 2024, **89**, 2637–2648.
- 66 Y. Yuan, F. Wu, J. Xu and X. Wu, *Angew. Chem., Int. Ed.*, 2020, **59**, 17055–17061.
- 67 F.-P. Wu and X.-F. Wu, *Chem. Sci.*, 2022, **13**, 4321–4326.
- 68 W. Ming, H. S. Soor, X. Liu, A. Trofimova, A. K. Yudin and T. B. Marder, *Chem. Soc. Rev.*, 2021, **50**, 12151–12188.
- 69 Y.-S. Zhu, Y.-L. Guo, Y.-Y. Zhu and B. Su, *J. Am. Chem. Soc.*, 2024, **146**, 32283–32291.
- 70 Y. Yuan, F. Ge, T. Yang and X.-F. Wu, *J. Catal.*, 2025, **450**, 116280.
- 71 S. Oishi, H. Kamitani, Y. Kodera, K. Watanabe, K. Kobayashi, T. Narumi, K. Tomita, H. Ohno, T. Naito, E. Kodama, M. Matsuoka and N. Fujii, *Org. Biomol. Chem.*, 2009, **7**, 2872.
- 72 A. M. Y. Suliman, E.-A. M. A. Ahmed, T.-J. Gong and Y. Fu, *Org. Lett.*, 2021, **23**, 3259–3263.
- 73 A. M. Y. Suliman, E.-A. M. A. Ahmed, T.-J. Gong and Y. Fu, *Chem. Commun.*, 2021, **57**, 6400–6403.
- 74 E.-A. M. A. Ahmed, H. Zhang, W.-G. Cao and T.-J. Gong, *Org. Lett.*, 2023, **25**, 9020–9024.
- 75 Y. Wang, J. Bai, Y. Yang, W. Zhao, Y. Liang, D. Wang, Y. Zhao and Z. Shi, *Chem. Sci.*, 2021, **12**, 3599–3607.
- 76 T. Wang, M. Wang, Y. Wang, M. Li, Y. Zheng, Q. Chen, Y. Zhao and Z. Shi, *Chem*, 2023, **9**, 130–142.



- 77 S. Li, H. Jiao, X.-Z. Shu and L. Wu, *Nat. Commun.*, 2024, **15**, 1846.
- 78 S. Li, C. Hu, L. Leo Liu and L. Wu, *Angew. Chem., Int. Ed.*, 2024, **63**, e202412368.
- 79 S. Kang, J. Lv, T. Wang, B. Wu, M. Wang and Z. Shi, *Nat. Commun.*, 2024, **15**, 7380.
- 80 Z. X. Giustra and S.-Y. Liu, *J. Am. Chem. Soc.*, 2018, **140**, 1184–1194.
- 81 H. Lyu, T. H. Tugwell, Z. Chen, G. A. Kukier, A. Turlik, Y. Wu, K. N. Houk, P. Liu and G. Dong, *Nat. Chem.*, 2024, **16**, 269–276.
- 82 A. D. J. Calow, D. Dailier and J. F. Bower, *J. Am. Chem. Soc.*, 2022, **144**, 11069–11074.
- 83 J. G. M. Morton, M. A. Dureen and D. W. Stephan, *Chem. Commun.*, 2010, **46**, 8947–8949.
- 84 D. Wang, X. Xue, K. N. Houk and Z. Shi, *Angew. Chem., Int. Ed.*, 2018, **57**, 16861–16865.
- 85 H. Kondo, S. Miyamura, K. Matsushita, H. Kato, C. Kobayashi, Arifin, K. Itami, D. Yokogawa and J. Yamaguchi, *J. Am. Chem. Soc.*, 2020, **142**, 11306–11313.

